Available online at www.sciencedirect.com
ScienceDirect
Sensors and Actuators A 142 (2008) 322–328
SENSORS AND ACTUATORS A PHYSICAL
www.elsevier.com/locate/sna

Localized-mass detection based on thin-film bulk acoustic wave resonators (FBAR): Area and mass location aspects

Humberto Campanella [a,b,*], Arantxa Uranga [b], Albert Romano-Rodríguez [c], Josep Montserrat [a], Gabriel Abadal [b], Nuria Barniol [b], Jaume Esteve [a]

[a] *Centro Nacional de Microelectrónica CNM-CSIC, Campus UAB, 08193 Bellaterra, Barcelona, Spain*
[b] *Universitat Autònoma de Barcelona, School of Engineering, Department of Electronics Engineering, Edifici Q, 08193 Bellaterra, Barcelona, Spain*
[c] *Universitat de Barcelona, Department of Electronics, c/Martí i Franquès, 1, Barcelona E-08028, Spain*

Received 29 September 2006; received in revised form 24 April 2007; accepted 8 May 2007
Available online 22 May 2007

Abstract

Localized-mass sensors using thin-film bulk acoustic resonators (FBAR) have been implemented for the study of sensitivity and possible configurations in biological applications. In a first experiment, a group of resonators are loaded with the same amount of mass but different contact areas, achieving responsivities as high as 10^{-19} g/Hz, and potential sensitivities in the order of 10^{-14} g. These numbers are at least one order of magnitude higher than those obtained for uniform thin-film loadings, although it is clear that sensitivity decreases with the area of the localized-mass. The current phase-noise levels and the quality factor of resonators would allow measuring frequency changes of 30 kHz – the minimum measured frequency shifting has been 500 kHz so far – due to a mass deposition of 9.0×10^{-15} g. In a second experiment, localized-loadings with the same mass are located in different positions of the top electrodes of the corresponding FBARs. It was found out that a location change of the mass in the electrode causes different magnitudes of frequency shifting. A discussion on these topics is opened, in order to define future applications and research lines concerning localized-mass sensing in FBARs.

Keywords: Thin-film bulk acoustic wave resonators; FBAR; BAW; Mass sensors; Responsivity and sensitivity of sensors

1. Introduction

The high sensitivity of thin-film bulk acoustic resonators (FBAR) makes this technology a suitable candidate for high-frequency applications, from radio-frequency to bio-molecular or chemical detection. Mass-sensing systems, in which quartz microbalances (QCM) have been a key technology, are now re-thought to be implemented with FBARs, taking advantage of its higher sensitivity compared to QCMs [1–4]. Specifically, the ability of FBARs to perform localized-mass detection was demonstrated in [1]. Other technological approaches, like nano-electro-mechanical (NEMS) resonators, have also proved to achieve a very high sensitivity in localized-mass detection applications [5–7].

In this work, different aspects of the location and contact area of the localized-mass deposition concerning the frequency response of the sensor are analyzed. "Localized-mass" refers to a material or compound deposited on the electrode of the FBAR, its dimensions being small enough compared to the electrode's area. In Fig. 1 a localized-mass deposited on the top electrode of a sample FBAR is shown. This load brings about down-shifting of the resonance frequency of the FBAR, by means of the so-called mass-loading effect. The loading is usually carried out through the growing or deposition of a thin-film material uniformly distributed on one electrode of the resonator, covering the whole active surface of the device. The fabrication technology determines the manner and the electrode on which the uniformly distributed mass is deposited. The mass loading affects the sensor's frequency response, lowering its resonance frequency (f_0). This frequency change Δf is proportional to the amount of deposited mass (Δm), and is evaluated in the Sauerbrey–Lostis equation [8] by: $\Delta f/f_0 = \Delta m/m_0$ (where m_0 is the unloaded resonator mass). This model is valid if Δm

* Corresponding author at: Centro Nacional de Microelectrónica CNM-CSIC, Campus UAB, 08193 Bellaterra, Barcelona, Spain. Tel.: +34 93 5947700; fax: +34 93 5801496.
E-mail address: humberto.campanella@cnm.es (H. Campanella).

0924-4247/$ – see front matter © 2007 Elsevier B.V. All rights reserved.
doi:10.1016/j.sna.2007.05.004

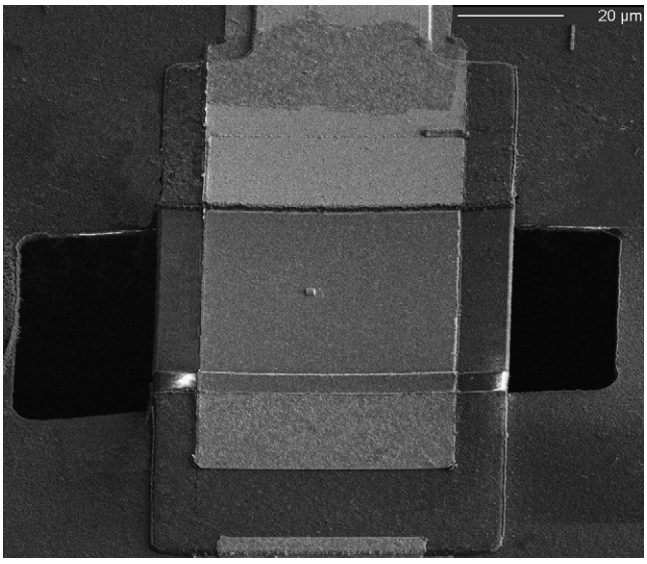

Fig. 1. Scanning electron microscope (SEM) image of a localized-mass deposited on the top electrode of the FBAR.

is less than 2% of m_0). Although the loading-mass is usually distributed on the overall area of the electrode through thin-film growing or PVD/CVD deposition, in this work loading is performed through the focused-ion-beam-assisted deposition of a localized-mass on the top electrode of the FBAR. In order to evaluate the mass-detector performance, two main parameters are used: responsivity and sensitivity. Mass responsivity R_m is defined as the change in frequency response per unit-mass change [Hz/g], but in certain cases it is more convenient to handle the inverse responsivity R_m^{-1} [g/Hz]. In this context, the minimum detectable mass change, or mass sensitivity, is calculated as the product $\Delta f \times R_m$ [9].

Due to the smaller size of an FBAR and the higher acoustic constants and densities of the materials used in their fabrication – usually AlN or ZnO – its mass sensitivity is highly improved in relation to the QCM [10,11]. As it was demonstrated in [1], localized-mass detectors based on FBAR exhibit improved responsivity and sensitivity – between one and two orders of magnitude – in comparison with distributed-mass detectors. However, the relationship between mass-sensing performance and location of deposited mass in the FBAR still needs further study. The contact area between mass and FBAR is another important parameter in the localized-mass detector performance. The impact of both aspects on the mass sensing is still to be analyzed, in order to broaden our knowledge about the localized-mass detector based on FBAR, and to develop future applications. For these reasons, this work is focused on AlN piezoelectric thin-films and on the exploration of different location and contact-area capabilities of localized-mass FBAR sensors.

2. FBAR technology and mass deposition

In order to implement a localized-mass sensor, a group of FBARs was designed, fabricated and mass-loaded. The FBAR sensors were implemented as a sandwiched aluminum nitride

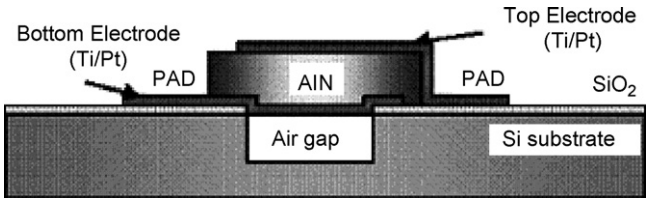

Fig. 2. Cross-sectional view schematic of the FBAR process. The FBAR is released by front-side micro-machining of the silicon substrate.

(AlN) membrane (1 μm-thick), sputtered on top of a platinum/titanium (Pt/Ti) layer (150/30 nm-thick), deposited on a silicon (Si) substrate, and released by front-side micromachining of Si to obtain a surface area of 50 μm × 70 μm for the top Ti/Pt electrode. With this configuration, the resonators' resonance frequency is around 2.3 GHz. A schematic of the FBAR process is depicted in Fig. 2. First, an isolating silicon oxide layer is deposited on top of the silicon substrate to provide electrical isolation and diminish rf losses. This layer is etched to provide a window to silicon when the releasing of the FBAR is performed in the last step of the process. Next, the bottom Pt/Ti electrode is deposited on the silicon-oxide layer. In this configuration, Ti serves as an adhesive layer for Pt, and the latter as a compatible substrate for the crystallographic structure of AlN. At the same time, the Pt/Ti layer serves as bottom electrode for the FBAR, and will be lifted-off to define the electrode area. Once this area has been defined, the AlN piezoelectric layer is deposited by rf sputtering and wet-etched in a TMAH-like solution. The top Pt/Ti electrode follows the same processing steps described for the bottom electrode. Finally, the releasing of the FBAR is performed by means of front-side reactive-ion etching (RIE) of Si, with a SF_6 and O_2 atmosphere in the RIE-machine-chamber. Considering this fabrication process, mass-loading is performed by depositing small bodies of a C/Pt/Ga composite on the top electrode of the FBAR (back-side bulk-micromachining processes often load the bottom electrode of FBAR-based sensors).

Deposition of mass-loads on selected areas of the top electrodes was performed inside a focused-ion-beam (FIB) machine, in order to test FBAR capabilities for localized-mass detection. For this purpose, a platinum-containing metalorganic precursor, injected in the sample's chamber, was decomposed by the ion-beam, giving rise to the localized deposition of an amorphous compound containing C, Pt and Ga (65, 27 and 8%, respectively) in the area scanned by the beam—its mass density being around 4 g/cm^3. A detailed description of this procedure can be found in [12]. First, we analyze the effect of mass and contact area of the load on the mass responsivity of the FBAR. In this paper, the expression "localized-mass" refers to a material or compound deposited on the electrode of the FBAR, the size of the mass being small compared to the electrode's area. Consequently, the deposition may be spatially selective to obtain the desired sensing configurations or working conditions. In these experiments, for example, the deposited-mass area for each one of the samples is always less than 0.7% of the electrode's surface (0.06% being the typical case). The characterization of scattering parameters, before and after the localized-mass deposition, was

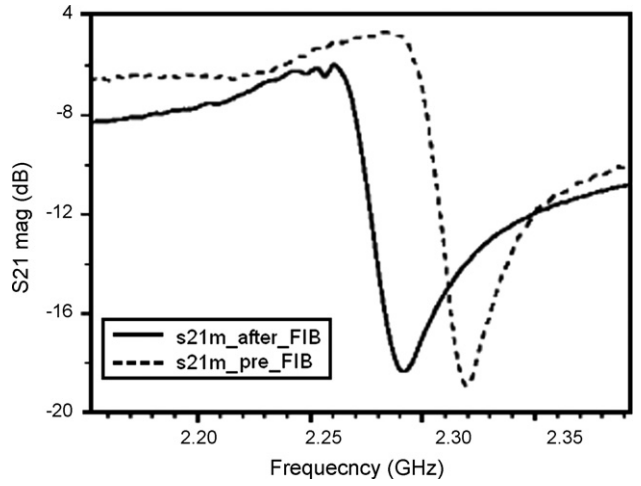

Fig. 3. Magnitude of the transmission scattering parameter S21 (dB) of an FBAR sensor, before (dotted line) and after FIB deposition (continuous line). Down-shifting of the resonance frequency is experimented after mass-loading of the FBAR's top electrode.

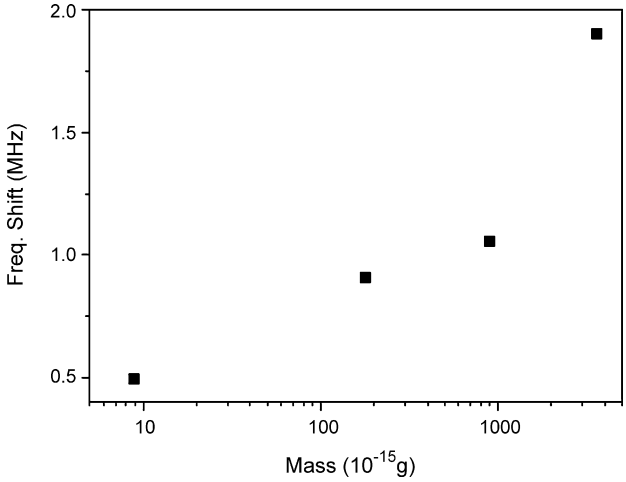

Fig. 4. Frequency shifting against mass-loading. Different masses with the same contact area (1.5 μm × 1.5 μm) are deposited on the center of the top electrode of the FBAR sensors.

carried out by means of an Agilent E5100A network analyzer and a co-planar-probe rf measurement station. Fig. 3 shows the magnitude of the S21 parameter for a rectangular-shaped FBAR, before and after deposition of a 25 μm^2-area square body corresponding to a mass of 4.97×10^{-15} g. Down-shifting of 28 MHz in the resonance frequency is observed. In Table 1, we specify the amount of mass, frequency shifting, mass responsivity and shifting factors for the loading of three resonators. The shifting factors help us understand the proportionality between mass and frequency change.

3. First study on responsivity: constant-area, localized-mass deposition

A first experiment, intended for the study of the mass dependency of responsivity, was carried out by depositing a 1.5 μm × 1.5 μm square-shaped composite of C/Pt/Ga on the geometric center of the top electrode of a group of resonators. A localized-mass of different thickness was deposited on each FBAR, in order to explore a range of masses. In this experiment we tested thicknesses of 1, 20, 100 and 400 nm, corresponding to a range of deposited masses between 9.0×10^{-15} and 3.6×10^{-12} g. In Fig. 4 the change of resonance frequency against the amount of deposited mass is plotted. Due to the wide range of deposited mass, the *x*-axis is presented in logarithmic scale.

In this figure, we can analyze responsivity [g/Hz]. In this experiment, the mass responsivity of the studied FBARs changes from tens of zg/Hz to ag/Hz. This value is competitive with respect to other NEMS technologies previously reported [5–7], and is specific for this mass-loading configuration. Later in this section, it will be shown that responsivity depends on both location and area of the localized-mass. Sensitivity [*g*] – minimum mass change that can be detected with the current measurement set-up and FBAR configuration – can be predicted by measuring the minimum frequency-shifting Δf that the set-up is able to detect, and by multiplying this value by the experimental mass responsivity. The set-up's minimum frequency shifting was found to be $\Delta f = 30$ kHz, calculating from the phase of the transmission S21 parameter. First, the phase noise is quantified from a zero-span acquisition, at the series resonance frequency (2.3 GHz). Next, the resulting value is divided by the phase slope, which is calculated from differentiation of the phase curve and evaluated at the series resonance frequency, thus obtaining a predicted average sensitivity value of 2.1×10^{-14} g. Although devices with the same configuration and similar performance and phase-noise conditions were used in these measurements, sensitivity values range from 5.0×10^{-16} to 5.0×10^{-14} g, for deposited masses in the range of 9.0×10^{-15} to 3.6×10^{-12} g. On the other hand, it is important to note that measuring of Δf allows the prediction of sensitivity, in order to determine the mass resolution of the system. Further experiments with the deposition of localized-mass on top of an FBAR, causing a frequency shifting around Δf, would allow to draw conclusions

Table 1
Mass responsivity of the FBAR for localized-mass deposition made with FIB

Mass deposited (g)	Frequency change (Hz)	Mass responsivity R_m (g/Hz)	Mass-shifting factor (m_0/m_i)	Frequency-shifting factor ($\Delta f_0/\Delta f_i$)
Δm_0: 4.9×10^{-15}	Δf_0: 2.86×10^7	1.74×10^{-22}	1	1
Δm_1: 1.8×10^{-15}	Δf_1: 7.09×10^6	2.54×10^{-22}	2.8	4.0
Δm_2: 9.0×10^{-16}	Δf_2: 3.15×10^6	2.85×10^{-22}	5.5	9.1

Three devices with a resonance frequency of 2.28 GHz are tested. The mass and frequency-shifting factors evidence a proportionality of frequency change with the amount of deposited mass.

about the actual mass sensitivity of the mass sensor. As for the sensitivity values obtained and the actual range of the deposited localized-mass, it can be deduced that the mass-sensitivity limit needs to be ultimately determined.

Concerning the incidence of FIB-deposition in the physical characteristics of the FBAR, additional experiments showed no appreciable electro-mechanical changes in the behavior of the FBAR. For example, resonance frequency and quality factor were not affected. This experiment was carried out by selecting some devices, which were exposed to the ion-beam, both for imaging and deposition of very small masses—not expected to change the resonance frequency. In both cases no significant changes in the electrical behavior of the FBAR were observed. In the following section, we study the area-dependent effects on the responsivity of localized-mass FBAR-sensors. In order to complement the first experiments, more testing was carried out with resonators on which loads having the same masses but different contact areas were deposited.

4. Second study on responsivity: constant-mass deposition and loading-area dependency

Deposition of the same amount of mass on the center of each resonator of a second group was performed, thus modifying both thickness and lateral size of the localized-loading to preserve the amount of deposited-mass. Initially, three loads with contact areas of 1.5 μm × 1.5 μm, 4.2 μm × 4.2 μm, and 6.0 μm × 6.0 μm and thicknesses of 400, 50, and 25 nm, respectively, were deposited—these geometrical configurations corresponding to a mass of 3.6×10^{-12} g. Taking a square of 1.5 μm × 1.5 μm as the reference area to calculate the relative area of deposited mass – the same as in the previous experiment – Fig. 5 illustrates the inverse relationship between frequency shifting and contact area of the loading-mass (in Fig. 5, "1" means a square-shaped unit-area of 1.5 μm × 1.5 μm, "10" is 10 times the unit-area, etc.). An alternative experiment was performed in order to analyze this find in greater detail by covering the whole surfaces of the top electrodes of several devices with a uniform thin-film of magnesium fluoride (MgF_2). For uniform-film deposition, responsivity was measured to be 1.50×10^{-17} g/Hz, which is worse than that for the localized-mass cases analyzed in the first experiment. On the other hand, the average responsivity of this constant-mass different-area experiment was 5.8×10^{-18} g/Hz, and the predicted sensitivity was 1.75×10^{-13} g. These numbers represent a decrease in responsivity and sensitivity of one order of magnitude in comparison with the first experiment, confirming the area-dependent nature of the sensor's performance.

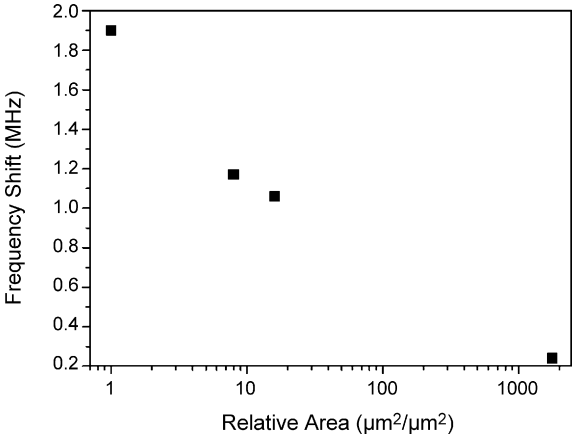

Fig. 5. Frequency shifting against normalized contact area of localized-mass deposited on top of the FBAR. In this experiment the amount of deposited mass is always the same (3.6×10^{-12} g).

5. Combined area-by-mass evaluation of responsivity

Although the first and second experiments demonstrate to a great extent the effects of the amount of mass and area on the responsivity of the FBAR sensor, a third experiment combining the configurations of previous experiments was carried out. This experiment – using samples with an arbitrary configuration of the loading mass – was designed with the aim of generalizing the results obtained before. For this purpose, loading with different masses and areas was performed in additional FBAR sensors. In order to provide the study with a rational comparison for the variety of configurations presented in this experiment, it was necessary to define a normalization parameter, as it had been done in the former experiments with mass and area. Here, the mass-by-area product normalizes the effect of the different configurations. First, in Fig. 6, the frequency shifting due to mass-loading is plotted against the mass-by-area product. In this figure the unitary value is a mass of 3.6×10^{-12} g with a contact area of 1.5 μm × 1.5 μm. The values in the *x*-axis are obtained from the mass-by-area product of the current sample. Due to the large range of mass and area configurations, the *x*-axis is presented in logarithmic scale.

As observed in Fig. 6, the relationship between mass and frequency shifting is non-linear when masses covering a range of several orders of magnitude are deposited. The mass-loading effect had been assumed to be linear for loading-masses in the

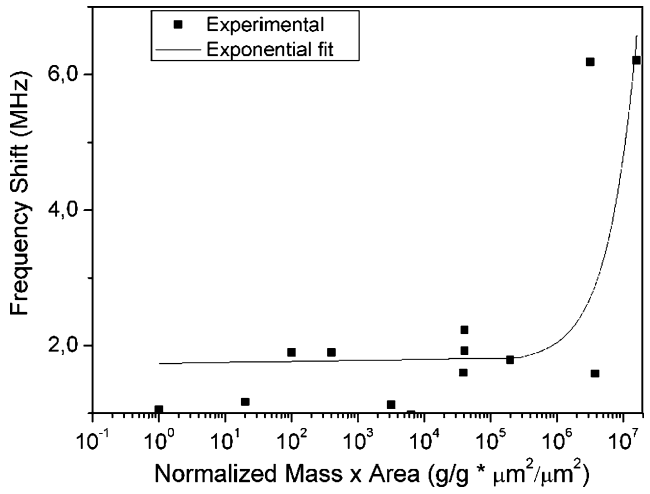

Fig. 6. Increase of frequency shifting with the normalized product of deposited mass-by-contact area. A mass of 3.6×10^{-12} g with a contact area of 1.5 μm × 1.5 μm is taken as the normalization reference.

same order of magnitude, as it was suggested by the plot in Fig. 5. Further information on this subject is given in Fig. 7a and b: (a) the normalized shifting of the resonance frequency against the normalized mass-by-area loading, and (b) the change of responsivity (g/Hz) against the normalized loading. Again, the large range of the mass-by-area product of deposited loads – several orders of magnitude – made the use of logarithmic scale in the *x*- and *y*-axes necessary. It is important to note that in Fig. 7a, the frequency shifting with respect to the mass-by-area product has been normalized (*y*-axis). In this way, we illustrate how big the change in the resonance frequency would be if the sensor had been loaded with a smaller load, given the current frequency-shifting behavior—due to larger loadings, both in mass and area.

What Fig. 7a actually indicates is that, when the FBAR sensor is loaded, resonance frequency shifts down less for bigger loads – both in area and mass – than for smaller ones. This fact can also be seen from the responsivity point of view. In Fig. 7b it is shown that responsivity worsens when the size or the mass of the localized-load are increased. Both interpretations offer different points of view of the localized-mass-loading effect.

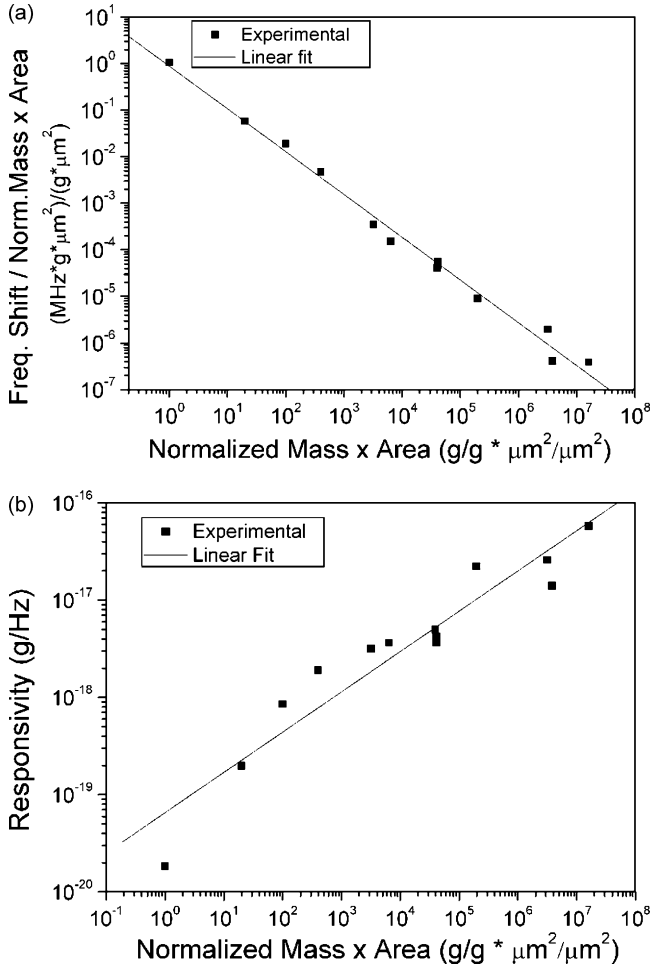

Fig. 7. Frequency shifting of the FBAR sensor for a variety of loadings: (a) relative frequency shifting against normalized mass-by-area; (b) responsivity [g/Hz] against normalized mass-by-area. Again, the reference mass is 3.6×10^{-12} g with a contact area of 1.5 μm × 1.5 μm.

6. Effect of the localized-mass-deposition location on responsivity

In the previous mass-loading experiments, the localized-load was always deposited on the center of the top electrode of resonators. Now, we present another experiment, carried out in order to test if responsivity and sensitivity are dependent on the region of the electrode on which the localized-mass is deposited. In this sense, this experiment might give information concerning responsivity and resonance mode-shaping as well. Given this scenario, the center of the resonator is taken as the geometric reference point for localized-mass deposition and observation of the related frequency shifting. Reference axes are also to be defined for deposition purposes. The schematic of Fig. 8 represents a top view of the FBAR, depicting the *center* of the resonator as a square-shaped spot, with three lines, one named *lateral* and two *diagonal*, crossing it. The *lateral* axis crosses the center of the FBAR, following the *y*-axis orientation (although it could also be defined in the *x*-axis orientation, in the context of this paper it will be understood only in the *y*-axis sense). Specifically, the localized-mass is deposited along this line, near the border of the electrode (far from the *center* and following the *y*-axis direction). The *diagonal* line connects the opposite corners of the electrode, crossing the *center*. The mass is deposited close to one of the corners and along the *diagonal* line.

Once the location of the localized-loads was defined, three depositions with the same mass and contact area were made on the *center*, and on the *lateral* and *diagonal* axes of the top electrodes of three different resonators. As a result of this experiment, the *center* of the FBAR proved to be the region of the electrode's geometry with the best responsivity, as it is detailed in Table 2. Previous work on atomic-force microscopy-based scanning of FBAR electrodes revealed that the amplitude of oscillation at resonance is related to the mode shape at this frequency. In [13], the vertical displacement of the FBAR's longitudinal resonance modes was bigger in the central region of the resonator. This could explain the higher sensitivity and responsivity values for this region found in this experiment. These results are also coherent with experimental data obtained for

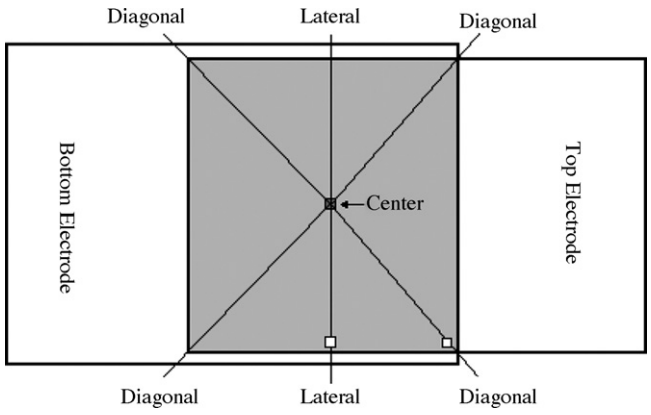

Fig. 8. Top-view schematic of the FBAR depicting the top electrode and axes for localized-mass deposition. A square spot, crossed by three lines, two named *lateral* and one *diagonal*, is drawn in the *center* of the resonator.

Table 2
Dependence of the FBAR responsivity on the axis of the top electrode on which the localized-mass is deposited

Region	Mass (estimated; g)	Δf (MHz)	Responsivity (g/Hz)
Center	3.6×10^{-12}	1.90	1.90×10^{-19}
Diagonal	3.6×10^{-12}	1.13	3.19×10^{-19}
Lateral	3.6×10^{-12}	0.98	3.65×10^{-19}

quartz crystal microbalances, in which localized silver spots are deposited on several positions along the diameter of quartz resonators [14]. Similar experiments have been carried out with crystal resonators immersed in liquid environments [15]. In these experiments mass sensitivity and amplitude distribution curves were found to follow a Gaussian function [16], the maximum being found at the center of the resonator's electrode. Since the mode shaping of resonance induces deformation in the vertical geometry of the FBAR, an explanation for improved sensitivity of the central region may be given in terms of different inertial fields generated on the surface of the electrode [17]. Regarding this explanation, the central region exhibits higher sensitivity, probably due to bigger acceleration forces – inertial field – in the center of the FBAR.

As commented in the above paragraph, the mass location effects on the resonance frequency could be understood in terms of the expected resonance modes of the mass-loaded FBAR. Nevertheless, this analysis could also be made from a different point of view: an extension of this experiment, in which localized-mass would be deposited on several resonators, could be used to study the resonance modes of our FBAR. This way, we could build the topography of the top electrode at resonance. Although this method is discrete – not the whole surface is analyzed but only selected points – it offers a good alternative to more complex microscopy-based methods studying FBAR topology at resonance [18–20]. The resonance mode of the FBAR affects responsivity as much as the size and mass of the load do. In the current stage of this work, a reference rectangular-shaped geometry has been the basis for the fabrication of tested resonators. Since the actual shape of resonance is strongly dependent on the lateral geometry of electrodes, future stages of this work would include an investigation of FBAR's responsivity as a function of the FBAR electrode's shaping.

7. Conclusions

Different experiments were conducted with FBAR-based localized-mass sensors, in order to study their responsivity and sensitivity in various localized-mass configurations. The achieved responsivities proved to be very competitive compared to NEMS technologies, specifically for the cases in which small-sized and small-mass loading is performed on the FBAR sensor. It was demonstrated that the responsivity of the localized-mass sensor changes when different-sized loads are deposited, thus opening a broad variety of size-based applications. Hence, the mass-loading configuration should be designed according to the target purpose. FBAR devices may be implemented as selective-particle sensors, which are of special interest in bio-molecular applications, like DNA and protein detection. Also, evaluation of the active-sensor area is an interesting subject to be studied in the future. Since responsivity is location-dependent, it determines both the application and design of the sensor. Future work should include further analytical and experimental evaluation of mode-shaping, based on topographic study of the electrode at resonance.

Acknowledgements

This work has been supported by *Seiko EPSON Corporation*, through its European branch *EPSON Europe Electronics GmbH* and EPSON's *Barcelona Research and Development Laboratory* (BRDL). H. Campanella would like to thank to C. Golden for fruitful discussions and helpful guidance.

References

[1] H. Campanella, J. Esteve, J. Montserrat, A. Uranga, G. Abadal, N. Barniol, A. Romano-Rodríguez, Localized and distributed mass detectors with high sensitivity based on thin-film bulk acoustic resonators, Appl. Phys. Lett. 89 (2006) 033507.
[2] M. Benetti, D. Cannatà, F. Di Pietrantonio, V. Foglietti, E. Verona, Microbalance chemical sensor based on thin-film bulk acoustic wave resonators, Appl. Phys. Lett. 87 (2005) 173504.
[3] M. Benetti, D. Cannatà, A. D'Amico, F. Di Pietrantonio, V. Foglietti, E. Verona, Thin film bulk acoustic wave resonator (TFBAR) gas sensor, in: Proc. IEEE Ultrason. Symp., Montreal, Canada, 24–27 August, 2004, pp. 1581–1584.
[4] H. Zhang, E.S. Kim, Micromachined acoustic resonant mass sensor, IEEE J. Microelectromech. Syst. 14 (2005) 699–706.
[5] E. Forsen, G. Abadal, S. Ghatnekar-Nilsson, J. Teva, J. Verd, R. Sandberg, W. Svendsen, F. Perez-Murano, J. Esteve, E. Figueras, F. Campabadal, L. Montelius, N. Barniol, A. Boisen, Ultrasensitive mass sensor fully integrated with complementary metal-oxide-semiconductor circuitry, Appl. Phys. Lett. 87 (2005) 043507.
[6] K.L. Ekinci, X.M.H. Huang, M.L. Roukes, Ultrasensitive nanoelectromechanical mass detection, Appl. Phys. Lett. 84 (2004) 4469–4471.
[7] B. Ilic, H.G. Craighead, S. Krylov, W. Senaratne, C. Ober, P. Neuzil, Attogram detection using nanoelectromechanical oscillators, J. Appl. Phys. 95 (2004) 3694–3703.
[8] G.Z. Sauerbrey, Verwendung von Schwingquarzen zur Wägung dünner Schichten und Microwägung, Z. Phys. 155 (1959) 206–222.
[9] K.L. Ekinci, Y.T. Yang, M.L. Roukes, Ultimate limits to inertial mass sensing based upon nanoelectromechanical systems, J. Appl. Phys. 95 (2004) 2682–2689.
[10] R. Gabl, H.-D. Feucht, H. Zeininger, G. Eckstein, M. Schreiter, R. Primig, D. Pitzer, W. Wersing, First results on label-free detection of DNA and protein molecules using a novel integrated sensor technology based on gravimetric detection principles, Biosens. Bioelectron. 19 (2004) 615–620.
[11] H. Zhang, M.S. Marma, E.S. Kim, C.E. McKenna, M.E. Thompson, A film bulk acoustic resonator in liquid environments, J. Micromech. Microeng. 15 (2005) 1911–1916.
[12] A. Vilà, F. Hernández-Ramírez, J. Rodríguez, O. Casals, A. Romano-Rodríguez, J.R. Morante, M. Abid, Fabrication of metallic contacts to nanometre-sized materials using a focused ion beam (FIB), Mater. Sci. Eng. C 26 (2006) 1063–1066.
[13] A. San Paulo, X. Liu, J. Bokor, Scanning acoustic force microscopy characterization of thermal expansion effects on the electromechanical properties of film bulk acoustic resonators, Appl. Phys. Lett. 86 (2005) 084102.
[14] V.M. Mecea, Loaded vibrating quartz sensors, Sens. Actuators A 40 (1994) 1–27.
[15] K.K. Kanazawa, J.G. Gordom, Frequency of a quartz microbalance in contact with liquid, Anal. Chem. 57 (1985) 1770–1771.

[16] B.A. Martin, H.E. Hager, Velocity profile on quartz crystals oscillating in liquids, J. Appl. Phys. 65 (1989) 2630–2635.
[17] V.M. Mecea, Is quartz crystal microbalance really a mass sensor? Sens. Actuators A 128 (2006) 270–277.
[18] K.L. Telschow, V.A. Deason, D.L. Cottle, J.D. Larson III, Full-field imaging of gigahertz film bulk acoustic resonator motion, IEEE T. Ultrason., Ferroelect., Freq. Control 50 (2003) 1279–1285.
[19] T. Makkonen, T. Pensala, J. Vartiainen, J. Knuuttila, J. Kaitila, M. Salomaa, Estimating material parameters in thin-film BAW resonators using measured dispersion curves, IEEE T. Ultrason., Ferroelect., Freq. Control 51 (2004) 42–51.
[20] A. San Paulo, X. Liu, J. Bokor, Atomic force microscopy characterization of electromechanical properties of RF acoustic bulk wave resonators, in: Proc. IEEE Intl. Conf. MEMS, Maastrich, The Netherlands, 25–29 January, 2004, pp. 169–172.

Biographies

Humberto Campanella received the BSc degree in electronics engineering from the Pontifical Javeriana University, Bogotá, Colombia in 1995, and the MSc in telecommunication systems from the Polytechnic University of Madrid, Spain in 1999. At this time, he pursues the PhD degree in electronics engineering. Since 2003, he is rf MEMS and analog IC engineer at the National Microelectronics Center CNM-CSIC, Barcelona, Spain. Before joining CNM-CSIC, he was with Alcatel-Bell Telephone, Celcaribe-Millicom Intl. Cellular, and Alcatel R&D-Intl. Division. Also, he was assistant professor and researcher at Universidad del Norte, Barranquilla, Colombia.

Arantxa Uranga was born in Burgos, Spain, in 1971. She received the degree in physics and electronics engineering from the Valladolid University, Spain, in 1994 and 1996, respectively, and the PhD degree in electronics engineering from the Autonomous University of Barcelona, Spain, in 2001. Since 1996, she has been with the Department of Electronics Engineering, Autonomous University of Barcelona, where she is a research scientist. Her research interests include the design of CMOS circuits for biomedical and rf applications.

Albert Romano-Rodríguez obtained his degree (1986) and PhD (1991) in physics from the University of Barcelona. From 1986 to 1988 he worked on electrical, optical and structural characterization of semiconductor materials and devices. From 1988 to 1991 he was with IMEC, Leuven, Belgium as a scientific collaborator. Back in Barcelona in 1991, he worked as a researcher at the University of Barcelona and in 1993 he was appointed Professor Titular (lecturer). From 2003 he has been strongly involved in the application of Focused Ion Beam techniques in nanotechnology with strong emphasis in the fabrication of nano-contacts to nanometer-sized materials.

Josep Montserrat obtained BS and PhD degrees in physics from the University of Barcelona in 1985 and 1991, respectively. In 1987 he joined the CNM-CSIC facilities in Bellaterra, Barcelona. He works as process engineer in the Clean Room Group. He is responsible for ion implantation and metallization areas. His main research interest is in silicon technology for the manufacture of CMOS integrated circuits, power devices and microelectronic sensors.

Gabriel Abadal received his degree in physics in 1991 and his PhD in electrical engineering in 1997 from the Universitat Autònoma de Barcelona. Since 2002 he is an associate professor in the Electronics Engineering Department of the Universitat Autònoma de Barcelona. His research interests is focused in the area of micro and nano-electromechanical systems (MEMS and NEMS) for sensor and rf communications applications, and their integration using CMOS standard technologies.

Nuria Barniol received the BS and PhD degrees in physics from the Universitat Autònoma de Barcelona, Spain, in 1987 and 1992, respectively. Currently, she is a professor with the Electronics Engineering Department at the same university. Her research interests are on the development of new analog integrated circuit structures for sensory and high-frequency systems in MEMS/NEMS applications.

Jaume Esteve was born in Parets del Vallés, Barcelona, Spain, in 1961. He received the PhD degree in physical electronics from the University of Barcelona in 1988. In 1990, he joined the Department of Silicon Technology and Microsystems, National Microelectronics Center CNM-CSIC, as a senior research scientist. His areas of interest include silicon micromachining technologies and their application to integrated sensors and actuators.